Available online at www.sciencedirect.com
SCIENCE DIRECT®
ELSEVIER
International Journal of Solids and Structures 43 (2006) 4757–4776
INTERNATIONAL JOURNAL OF SOLIDS and STRUCTURES
www.elsevier.com/locate/ijsolstr

Layup optimization with GA for tapered laminates with internal plydrops

Seung Yun Rhee [a], Maenghyo Cho [a], Heung Soo Kim [b,*]

[a] *School of Mechanical and Aerospace Engineering, Seoul National University, San 56-1, Shillim-Dong, Kwanak-Gu, Seoul 151-744, Republic of Korea*
[b] *Department of Mechanical Engineering, Inha University, 253 Yong-Hyun Dong, Nam-Ku, Incheon, 402-751, Republic of Korea*

Received 30 March 2005; received in revised form 1 July 2005
Available online 8 September 2005

Abstract

Layup optimization of the maximum strength of laminated composites with internal ply-drops is performed by genetic algorithm (GA). Interlaminar stresses are considered in estimating the strength of laminates and calculated by the stress function based complementary virtual work principle. Out-of-plane stress functions are expanded in terms of harmonic series through the thickness direction and initially satisfied the traction free boundary conditions of laminates automatically. As the number of expansion terms is increased, stress concentration near the dropped plies is predicted with better accuracy. Since the proposed analysis is relatively simple and efficient in the prediction of interlaminar stress concentration near the ply-drops, the layup optimization of composite laminates with dropped plies considering interlaminar strength can be easily performed by GA. In the formulation of genetic algorithm, a repair strategy is adopted to satisfy given constraints and multiple elitism scheme is implemented to efficiently find multiple global optima or near-optima.

Keywords: Internal ply-drops; Interlaminar stress; Genetic algorithm; Repair strategy; Multiple elitism

1. Introduction

To save weight when loads are non-uniform, the composite laminates with tapered thickness have commonly been manufactured by terminating, or dropping internal plies within the laminates. This is an important method of tailoring stiffness in structures made from advanced composite materials. For example, it is

* Corresponding author. Tel.: +82 32 860 8256; fax: +82 32 868 1716.
E-mail addresses: syrhee8@snu.ac.kr (S.Y. Rhee), mhcho@snu.ac.kr (M. Cho), heungsookim@inha.ac.kr (H.S. Kim).

0020-7683/$ - see front matter © 2005 Elsevier Ltd. All rights reserved.
doi:10.1016/j.ijsolstr.2005.07.015

recommended that there should be ply-drops in aircraft wing skins, in composite flexbeams of helicopter rotor hubs, and near field joints in solid rocket boosters. Tapered composite structures create geometry and material discontinuities near dropped plies of composite laminates, which cause high stress concentration, or singularity. The stress concentration initiates failure of the laminates and thus the prediction of interlaminar stresses at the dropped plies is required in solving the optimization problem of a layup design.

Stress analysis near the dropped plies is similar to that of free-edge problem. Numerous research efforts have been made to resolve serious stress concentration/singularity near the free edges and near the dropped plies of composite laminates. However, since the difficulties occur during the process of obtaining the exact singular elasticity solutions, approximate methods have been pursued which are based on numerical or analytical approaches. Although recently developed numerical methods consist of either finite element methods or boundary integral methods, simple and reliable analytical methods are preferred in the preliminary design stage since they facilitate parametric study. After Pipes and Pagano (1970) proposed free-edge interlaminar stress analysis, linear elastic models and simple regular stress function-based approximation methods have been proposed for interlaminar stress problems with free edges. Present analysis method for tapered laminates is based on the stress function-based variational method of free-edge interlaminar stresses proposed by Cho and Yoon (1999) and Cho and Kim (2000). In the case of the presence of free edge at the boundary, the layup optimization considering bounded uncertainty of material properties were conducted by Cho and Rhee (2003, 2004).

Fish and Lee (1989) showed the delamination effect of interlaminar stresses for laminates with internal ply-drops. To analyze interlaminar stresses, Fish and Lee used 2-D finite element method. Botting et al. (1996) reported the effect of ply-drop by using FEM and experiments. They used 3-D solid finite element to analyze interlaminar stresses. Mukherjee and Varughese (1999) proposed global-local scheme for the reduction of degrees of freedom. However, FEM approach requires large amount of computer resources. Harrison and Johnson (1996) proposed a mixed variational formulation for reliable approximations of interlaminar stresses. A mixed formulation has an advantage in describing displacement-prescribed boundary conditions and displacement continuity conditions at the interfaces between layers but it has too many primary variables. On the other hand, a stress function-based variational method shows simple and efficient approximation in the prediction of interlaminar stresses only with stress variables. The present study is based on complementary strain energy principle with stress variables only. It is essential in the optimization procedure to reduce computing time of objective function which is the strength of laminates in the present study.

In laminated composite structures, the layups of laminates can be arranged for the lightweight and/or high performance of composite structures. In most structural designs using composite laminates, laminates are restricted to some discrete sets of ply orientation angles such as $0°$, $\pm 45°$ and $90°$. This practical manufacturing point of view requires the discretized optimization methodology for the layup design problem. Genetic algorithm (GA) is considered as a powerful methodology for the discretized problems in which the gradient of the objective functions is difficult to obtain. A considerable number of researches in design optimization of composite structures have reported the employment of genetic algorithm. Le Riche and Haftka (1993) proposed a genetic algorithm to optimize the stacking sequence of composite laminate for maximum buckling load. A recessive-gene-like repair strategy was introduced by Todoroki and Haftka (1998) to handle given constraints efficiently. Recently, Soremekun et al. (2001) applied the generalized elitist selection (GES) scheme to the problems with many global optima and near-optima showing performance very close to optimal. Because of random nature of GA, they easily produce alternative optima in repeated runs. This property is particularly important in layup optimization because widely different layups can have very similar performance.

In the tapered composite laminates, common design practice is weight minimization of laminates with required stiffness constraints. However, in the present study, we perform the layup optimization for the maximum strength of laminated composites with internal ply-drops by genetic algorithm (GA) with a repair strategy and multiple elitism.

2. Interlaminar stress analysis based on the complementary strain energy principle

2.1. Stress function based analysis

The geometry of composite laminates with internal ply-drops is given in Fig. 1. The laminate consists of orthotropic materials. The plies have arbitrary angles relative to the x axis. The linear elastic constitutive equations are assumed in each ply and they are expressed in the following form:

$$\begin{Bmatrix} \varepsilon_1 \\ \varepsilon_2 \\ \varepsilon_3 \\ \varepsilon_4 \\ \varepsilon_5 \\ \varepsilon_6 \end{Bmatrix} = \begin{bmatrix} S_{11} & S_{12} & S_{13} & 0 & 0 & S_{16} \\ S_{12} & S_{22} & S_{23} & 0 & 0 & S_{26} \\ S_{13} & S_{23} & S_{33} & 0 & 0 & S_{36} \\ 0 & 0 & 0 & S_{44} & S_{45} & 0 \\ 0 & 0 & 0 & S_{45} & S_{55} & 0 \\ S_{16} & S_{26} & S_{36} & 0 & 0 & S_{66} \end{bmatrix} \begin{Bmatrix} \sigma_1 \\ \sigma_2 \\ \sigma_3 \\ \sigma_4 \\ \sigma_5 \\ \sigma_6 \end{Bmatrix} + \begin{Bmatrix} \alpha_1 \\ \alpha_2 \\ \alpha_3 \\ 0 \\ 0 \\ \alpha_6 \end{Bmatrix} \Delta T \tag{1}$$

From the first row of Eq. (1), following relationship is obtained:

$$\sigma_1 = (\varepsilon_1 - \alpha_1 \Delta T - S_{1j}\sigma_j)/S_{11} \tag{2}$$

Substituting Eq. (2) into Eq. (1), all the strains can be expressed as

$$\varepsilon_i = \hat{S}_{ij}\alpha_j + \frac{S_{i1}}{S_{11}}\varepsilon_1 + \hat{\alpha}_i \Delta T \quad (i,j = 2,3,4,5,6) \tag{3}$$

where

$$\hat{S}_{ij} = S_{ij} - \frac{S_{1i}S_{1j}}{S_{11}}, \quad \hat{\alpha}_i = \alpha_i - \frac{S_{1i}}{S_{11}}\alpha_1 \tag{4}$$

Generalized plane strain states are assumed in the x direction and Lekhnitskii stress functions (1963) are introduced to satisfy pointwise equilibrium equations automatically. These stress functions can be assumed as homogeneous parts and particular parts as follows:

$$F = F_h + F_p = \sum_{i=1}^{n} f_i(y)g_i(y,z) + \frac{N_{yy}z^2}{2H(y)}, \quad \psi = \psi_h + \psi_p = \sum_{i=1}^{n} p_i(y)g_i(y,z)_{,z} + \frac{N_{xy}z}{H(y)} \tag{5}$$

where f_i and p_i are in-plane stress functions and g_i is out-of-plane stress function which can describe tapered geometry of laminates. Terms, N_{yy} and N_{xy}, are longitudinal compression and in-plane shear, respectively. Function $H(y)$ is the thickness of tapered laminates and can be expressed as follows:

$$H(y) = z_t(y) - z_b(y) \tag{6}$$

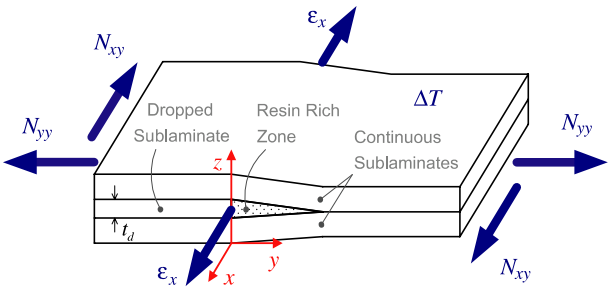

Fig. 1. Geometry of composite laminates with dropped plies.

where z_t and z_b are functions of the top and bottom curves. All stress components are expressed in terms of stress functions as follows:

$$\sigma_2(\sigma_{yy}) = \frac{\partial^2 F}{\partial z^2}, \quad \sigma_3(\sigma_{zz}) = \frac{\partial^2 F}{\partial y^2}, \quad \sigma_4(\sigma_{yz}) = -\frac{\partial^2 F}{\partial y \partial z}, \quad \sigma_5(\sigma_{zx}) = -\frac{\partial \psi}{\partial y}, \quad \sigma_6(\sigma_{xy}) = \frac{\partial \psi}{\partial z} \tag{7}$$

Homogeneous parts of stress functions are enough to analyze interlaminar stresses under thermal loading. However, it is not enough to analyze interlaminar stresses under mechanical loadings. Therefore, the particular parts of stress functions are introduced to describe the effects of mechanical loadings. In the present model, out-of-plane stress distributions are governed by the homogeneous parts of stress functions. By substituting Eq. (5) into Eq. (7), the stresses are expressed in terms of stress functions as follows:

$$\begin{cases} \sigma_2 = f_i g_{i,zz} + \frac{N_{yy}}{H}, \quad \sigma_3 = f_{i,yy} g_i + 2 f_{i,y} g_{i,y} + f_i g_{i,yy} + \frac{N_{yy} z^2 H_{,y}^2}{H^3} \\ \sigma_4 = -f_{i,y} g_{i,z} - f_i g_{i,yz} + \frac{N_{yy} z H_{,y}}{H^2}, \quad \sigma_5 = -p_{i,y} g_{i,z} - p_i g_{i,yz} + \frac{N_{xy} z H_{,y}}{H^2} \\ \sigma_6 = -p_i g_{i,zz} + \frac{N_{xy}}{H} \end{cases} \tag{8}$$

The change of tapered thickness is assumed to be linear to make the formulation simple. Then, second derivative of thickness is zero and interlaminar normal stress is expressed in a simple form as shown above.

Schematic view of tapered laminates is shown in Fig. 2. Let n and t denote normal and tangential directions to the curved boundary. By applying the usual stress transformation rule to the preceding results, we obtain

$$\begin{cases} \sigma_{nn} = \sigma_2 \sin^2\gamma_k + \sigma_3 \cos^2\gamma_k - 2\sigma_4 \sin\gamma_k \cos\gamma_k = \sigma_{nn}^h + \sigma_{nn}^p \\ \sigma_{tn} = (\sigma_2 - \sigma_3)\sin\gamma_k \cos\gamma_k + \sigma_4(\cos^2\gamma_k - \sin^2\gamma_k) = \sigma_{tn}^h + \sigma_{tn}^p \\ \sigma_{xn} = \sigma_5 \cos\gamma_k - \sigma_6 \sin\gamma_k = \sigma_{xn}^h + \sigma_{xn}^p \end{cases} \tag{9}$$

Since these interlaminar stresses are composed of homogeneous and particular parts of stress functions, interlaminar stresses can be divided into homogeneous and particular parts as shown in Eq. (9).

The schematic view of tapered laminates shows traction free boundary conditions at the top and bottom surfaces, C_s. When mechanical loading is applied, edge boundaries, C_e, are prescribed by stresses. Therefore, the boundary conditions along boundaries, C_e and C_s, can be expressed as follows:

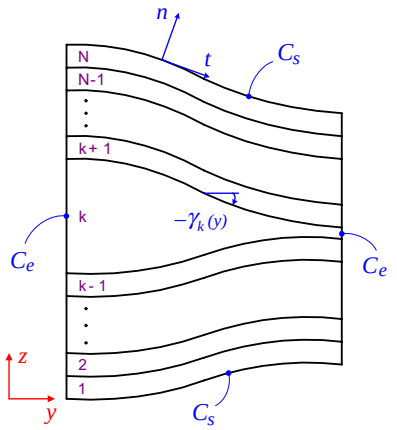

Fig. 2. Schematic view of tapered laminates.

$$\begin{cases} \sigma_2, \sigma_4, \sigma_6 = \text{prescribed on } C_e(\text{edge boundaries}) \\ \sigma_{nn} = \sigma_{nt} = \sigma_{xn} = 0 \text{ on } C_s(\text{top and bottom surface}) \end{cases} \tag{10}$$

From C_s boundary conditions, the initially assumed out-of-plane functions must satisfy traction free boundary conditions at the top and bottom surfaces, i.e. the stress functions and their first and second derivatives have to be zero in those regions. Therefore, the following harmonic function is assumed as the out-of-plane stress function:

$$g_i(y,z) = \frac{1}{i}\sin\{i\pi\eta\} - \frac{1}{i+2}\sin\{(i+2)\pi\eta\} \quad (i = 1,2,\ldots,n) \tag{11}$$

where

$$\eta = \frac{z - z_b(y)}{z_t(y) - z_b(y)} \tag{12}$$

To avoid trivial case, even functions of g_i are selected. From Eq. (11), homogeneous parts of interlaminar stresses automatically satisfy C_s boundary conditions.

Trigonometric values should be expressed in terms of thickness location z to verify whether particular parts of interlaminar stresses satisfy C_s boundary conditions or not. The slope of each interface, γ_k, as shown in Fig. 2 is given as follows:

$$\tan\gamma_k = z_{k,y} \tag{13}$$

From Eq. (13), one can get cosine and sine values as follows:

$$\cos\gamma_k = \frac{1}{\sqrt{1+z_{k,y}^2}}, \quad \sin\gamma_k = \frac{z_{k,y}}{\sqrt{1+z_{k,y}^2}} \tag{14}$$

Substituting Eq. (14) into Eq. (9), the particular parts of interlaminar stresses at each interface are expressed as follows:

$$\begin{aligned} \sigma_{nn}^p &= \frac{N_{yy}(z_k H_{,y} - H z_{k,y})^2}{H^3(1+z_{k,y}^2)}, \quad \sigma_{xn}^p = \frac{N_{xy}(z_k H_{,y} - H z_{k,y})}{H^2\sqrt{1+z_{k,y}^2}} \\ \sigma_{tn}^p &= \frac{N_{yy}\{-z_{k,y}H^2 + z_k^2 z_{k,y} H_{,y}^2 - z_k H H_{,y}(-1+z_{k,y}^2)\}^2}{H^3(1+z_{k,y}^2)} \end{aligned} \tag{15}$$

In this study, eccentricity of geometry was investigated as shown in Fig. 3. In the case without eccentricity, the horizontal coordinate is located at the mid surface of laminates as shown in Fig. 3a. Then, top and bottom surface location has following relationships:

$$z_b = -z_t, \quad z_b' = -z_t' \tag{16}$$

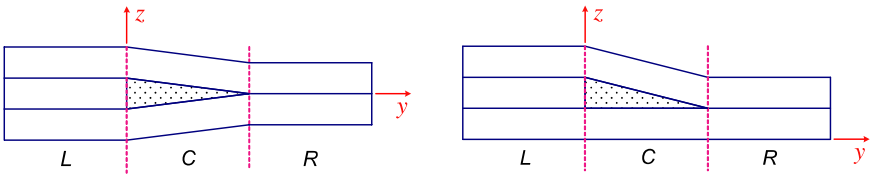

(a) without Eccentricity (b) with Eccentricity

Fig. 3. Laminates without (a) and with (b) eccentricity in the middle surface.

In the case with eccentricity, the horizontal coordinate is located at the bottom surface of laminates as shown in Fig. 3b. Then, bottom surface location and its first derivative are zero.

$$z_b = z'_b = 0 \tag{17}$$

From Eqs. (16) and (17), particular parts of interlaminar stresses can satisfy traction free boundary conditions at top and bottom surfaces. From these procedures, the assumed stress functions satisfy all C_s boundary conditions.

The governing equations in terms of in-plane stress functions are obtained by taking the stationary value of complementary strain energy.

$$\delta U = \int\int \varepsilon_i \delta\sigma_i \,\mathrm{d}\eta\,\mathrm{d}\xi = \int\int \left(\hat{S}_{ij}\sigma_j + \frac{S_{i1}}{S_{11}}\varepsilon_1 + \hat{\alpha}_i \Delta T\right)\delta\sigma_i \,\mathrm{d}y\,\mathrm{d}z \tag{18}$$

Next, Eq. (8) is substituted into Eq. (18) and repeated integration by parts is applied to obtain

$$\begin{aligned}&\int [a_{ij}^{(4)} f_{j,yyy} + a_{ij}^{(3)} f_{j,yyy} + a_{ij}^{(2)} f_{j,yy} + a_{ij}^{(1)} f_{j,y} + a_{ij}^{(0)} f_j + b_{ij}^{(2)} p_{j,yy} + b_{ij}^{(1)} p_{j,y} + b_{ij}^{(0)} p_j + r_i]\delta f_i \,\mathrm{d}y \\ &\quad + \int [c_{ij}^{(2)} f_{j,yy} + c_{ij}^{(1)} f_{j,y} + c_{ij}^{(0)} f_j + d_{ij}^{(2)} p_{j,yy} + d_{ij}^{(1)} p_{j,y} + d_{ij}^{(0)} p_j + s_i]\delta p_i \,\mathrm{d}y = 0\end{aligned} \tag{19}$$

where

$$\begin{aligned}
a_{ij}^{(4)} &= \int \hat{S}_{33} g_i g_j \,\mathrm{d}z, \qquad a_{ij}^{(3)} = \int 4\hat{S}_{33} g_i g_{j,y} \,\mathrm{d}z \\
a_{ij}^{(2)} &= \int \hat{S}_{23}(g_{i,zz} g_j + g_i g_{j,zz}) \,\mathrm{d}z + \int 6\hat{S}_{33} g_i g_{j,yy} \,\mathrm{d}z - \int \hat{S}_{44} g_{i,z} g_{j,z} \,\mathrm{d}z \\
a_{ij}^{(1)} &= \int 2\hat{S}_{23}(g_{i,zz} g_{j,y} + g_i g_{j,yzz}) \,\mathrm{d}z + \int 4\hat{S}_{33} g_i g_{j,yyy} \,\mathrm{d}z - \int 2\hat{S}_{44} g_{i,z} g_{j,yz} \,\mathrm{d}z \\
a_{ij}^{(0)} &= \int \hat{S}_{22} g_{i,zz} g_{j,zz} \,\mathrm{d}z + \int \hat{S}_{23}(g_{i,zz} g_{j,yy} + g_i g_{j,yyzz}) \,\mathrm{d}z + \int \hat{S}_{33} g_i g_{j,yyyy} \,\mathrm{d}z - \int \hat{S}_{44} g_{i,z} g_{j,yyz} \,\mathrm{d}z \\
b_{ij}^{(2)} &= \int \hat{S}_{36} g_i g_{j,zz} \,\mathrm{d}z - \int \hat{S}_{45} g_{i,z} g_{j,z} \,\mathrm{d}z, \qquad b_{ij}^{(1)} = \int 2\hat{S}_{36} g_i g_{j,yzz} \,\mathrm{d}z - \int 2\hat{S}_{45} g_{i,z} g_{j,yz} \,\mathrm{d}z \\
b_{ij}^{(0)} &= \int \hat{S}_{26} g_{i,zz} g_{j,zz} \,\mathrm{d}z + \int \hat{S}_{36} g_i g_{j,yyzz} \,\mathrm{d}z - \int \hat{S}_{45} g_{i,z} g_{j,yyz} \,\mathrm{d}z \\
c_{ij}^{(2)} &= \int \hat{S}_{36} g_{i,zz} g_j \,\mathrm{d}z - \int \hat{S}_{45} g_{i,z} g_{j,z} \,\mathrm{d}z, \qquad c_{ij}^{(1)} = \int 2\hat{S}_{36} g_{i,zz} g_{j,y} \,\mathrm{d}z - \int 2\hat{S}_{45} g_{i,z} g_{j,yz} \,\mathrm{d}z \\
c_{ij}^{(0)} &= \int \hat{S}_{26} g_{i,zz} g_{j,zz} \,\mathrm{d}z + \int \hat{S}_{36} g_{j,zz} g_{j,yy} \,\mathrm{d}z - \int \hat{S}_{45} g_{i,z} g_{j,yyz} \,\mathrm{d}z \\
d_{ij}^{(2)} &= \int \hat{S}_{55} g_{i,z} g_{j,z} \,\mathrm{d}z, \qquad d_{ij}^{(1)} = -\int 2\hat{S}_{55} g_{i,z} g_{j,yz} \,\mathrm{d}z \\
d_{ij}^{(0)} &= \int \hat{S}_{66} g_{i,zz} g_{j,zz} \,\mathrm{d}z + \int \hat{S}_{55} g_{i,z} g_{j,yyz} \,\mathrm{d}z
\end{aligned} \tag{20-1}$$

$$\begin{aligned}
r_i = \int \Bigg[&\left(\frac{S_{12}}{S_{11}}\varepsilon_1 + \hat{\alpha}_2 \Delta T\right) g_{i,zz} + \frac{N_{xy}}{H}\left\{\hat{S}_{26} g_{i,zz} + \frac{2H_{,y}^2}{H^2}(\hat{S}_{36} g_i - \hat{S}_{45} z g_{i,z})\right\} \\
&+ \frac{N_{yy}}{H}\left\{\hat{S}_{22} g_{i,zz} + \frac{H_{,y}^2}{H^2}(2\hat{S}_{23} g_i - 2\hat{S}_{44} z g_{i,z} + \hat{S}_{23} z^2 g_{i,zz}) + \frac{12H_{,y}^4}{H^4}\hat{S}_{33} Z^2 g_i\right\}\Bigg] \mathrm{d}z
\end{aligned}$$

$$S_i = \int \left[\left(\frac{S_{16}}{S_{11}} \varepsilon_1 + \hat{\alpha}_6 \Delta T \right) g_{i,zz} + \frac{N_{xy}}{H} \left(\hat{S}_{66} g_{i,zz} - \frac{2H_{,y}^2}{H^2} \hat{S}_{55} z g_{i,z} \right) + \frac{N_{yy}}{H} \left\{ \hat{S}_{26} g_{i,zz} + \frac{H_{,y}^2}{H^2} (\hat{S}_{36} z^2 g_{i,zz} - 2\hat{S}_{45} z g_{i,z}) \right\} \right] \mathrm{d}z \tag{20-2}$$

These $2n$ coupled fourth and second order ordinary differential equations can be solved by $6n$ boundary values. From C_e boundary conditions, one can get boundary values of f_i, $f_{i,y}$ and p_i. Integrated values of three stresses are prescribed at each edge boundary. To get $6n$ boundary values, weighted-averaged stress conditions are applied for representing CLT stress distribution.

$$\begin{aligned} \int \sigma_2 g_{j,zz} \, \mathrm{d}z &= \int \left(f_i g_{i,zz} + \frac{N_{yy}}{H} \right) g_{j,zz} \, \mathrm{d}z = \int \sigma_2^{\mathrm{CLT}} g_{j,zz} \, \mathrm{d}z \\ \int \sigma_4 g_{j,zz} \, \mathrm{d}z &= \int \left(-f_i g_{i,z} - f_i g_{i,yz} + \frac{N_{yy} z H_{,y}}{H^2} \right) g_{j,z} \, \mathrm{d}z = \int \sigma_4^{\mathrm{CLT}} g_{j,z} \, \mathrm{d}z = 0 \\ \int \sigma_6 g_{j,zz} \, \mathrm{d}z &= \int \left(p_i g_{i,zz} + \frac{N_{xy}}{H} \right) g_{j,zz} \, \mathrm{d}z = \int \sigma_6^{\mathrm{CLT}} g_{j,zz} \, \mathrm{d}z \end{aligned} \tag{21}$$

where σ_2^{CLT} and σ_6^{CLT} can be obtained from classical lamination theory (CLT).

We applied the forward, central and backward methods in order to compute derivatives in finite difference schemes. Selection of scheme among forward, central and backward difference schemes depends on where the computation region belongs to among L, C and R regions shown in Fig. 3.

To measure the tendency of laminates to be delaminated, the delamination fraction proposed by Harrison and Johnson (1996) is employed in order to account for the combined effect of each stress component.

$$F_D = \sqrt{\left(\frac{\sigma_{nn}}{Z_T} \right)^2 + \left(\frac{\sigma_{tn}}{Z_{S1}} \right)^2 + \left(\frac{\sigma_{xn}}{Z_{S2}} \right)^2} \tag{22}$$

where σ_{nn} is the interlaminar normal stress, δ_{tn} and δ_{xn} are the interlaminar shear stress, and Z_T, Z_{S1} and Z_{S2} are the allowable interlaminar stresses. The onset of delamination occurs when $F_D \geqslant 1$.

2.2. Examples of the analysis

In these examples, the two continuous sublaminates have the same eight-ply quasi-isotropic $[\pm 45/0/90]_s$ layup and the dropped sublaminate contains $[90_4]$ layup. Material systems is AS4/3502 graphite/epoxy (Harrison and Johnson, 1996) and its material properties and those for the net resin are given as follows:

$$\begin{aligned} &E_1 = 128 \text{ GPa}, \quad E_2 = E_3 = 11.3 \text{ GPa}, \quad G_{12} = G_13 = 6.0 \text{ GPa}, \quad G_{23} = 3.38 \text{ GPa}, \\ &v_{12} = v_{13} = 0.3, \quad v_{23} = 0.35, \quad E_{\text{resin}} = 3.45 \text{ GPa}, \quad v_{\text{resin}} = 0.41 \end{aligned} \tag{23}$$

and the allowable interlaminar stresses are

$$Z_{s1} = Z_{s2} = 93.08 \text{ MPa}, \quad Z_T = 51.99 \text{ MPa} \tag{24}$$

First, the solution convergence of the present method is studied. The distribution of interlaminar shear stress under longitudinal compression is shown in Fig. 4. The longitudinal direction is normalized by the thickness of the dropped sublaminate (t_d). Interlaminar shear stress is quickly converged as the number of initially assumed out-of-plane stress functions is increased. It is observed that four-term approximation provides converged interlaminar stress. Therefore, four-term approximation is conducted for the strength analysis in the present paper. Interlaminar stresses are concentrated at the beginning point of dropped zone

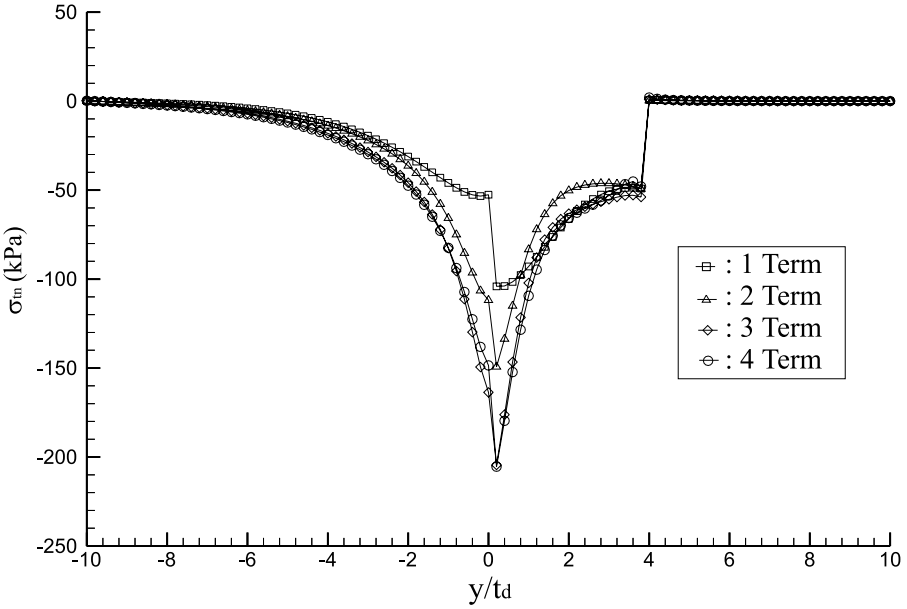

Fig. 4. Convergence of shear stress (σ_{tn}) along the upper interface of four 90° dropped plies ($N_{yy} = -1$ kN/m).

and disappear in the distance of about two times of dropped zone length. This is the same phenomenon observed at the free edge of laminated structure (Pipes and Pagano, 1970). Therefore, it is expected that the failure will occur at the beginning point of dropped zone.

Fig. 5 shows comparable results of delamination fractions along the upper interface of four 90° dropped plies under the same load. Delamination fraction shows averaged delamination effect of interlaminar stresses. Harrison and Johnson (1996) used a mixed variational formulation to predict interlaminar stresses near the dropped plies. The number of primary variables of the mixed formulation is $23m$, where m is the

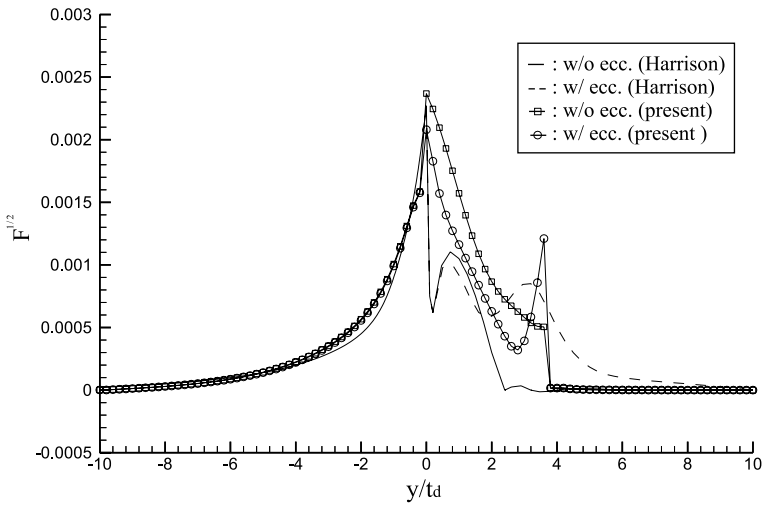

Fig. 5. Delamination fraction along the upper interface of four 90° dropped plies ($N_{yy} = -1$ kN/m).

number of averaged sublaminates, whereas that of present method is $2n$, where n is the number of initially assumed basis functions. From this comparison of the number of primary variables, one can find that the present method is simpler and more efficient than the mixed formulation. It is observed that the present results show higher concentrations than those obtained by the mixed formulation. Maximum values of failure index show good correlations between present method and Harrison's. This provides that the present stress function-based approximation method can be used as a strength design tool of tapered laminates with internal ply-drops.

3. Genetic algorithm (GA)

3.1. Outline of GA scheme

The flowchart of GA is illustrated in Fig. 6. To represent the ply angles in a layup as genes (in a chromosome), three numbers are introduced with each gene having one of the values of 0, 1 or 2. The gene-0 and gene-2 correspond to 0° and 90° plies respectively. The first (outermost), third, fifth, etc. occurrences of gene-1 correspond to +45° while even-number occurrences correspond to −45°. Herein only half of the plies are represented by the chromosome due to the symmetry of laminates.

After selection, a crossover, which uses one cut-point but is different from a simple crossover, is conducted with a probability value of P_{cr}. One random cut-point is chosen first and two different schemes are applied according to the position of the cut-point. When its position is on the continuous sublaminate, the offspring is generated by combining the left segment of one parent with the right segment of the other parent (Fig. 7a). But when the position is on the dropped sublaminate, the parents exchange the left part of cut-point in dropped plies (Fig. 7b).

A recessive-gene-like repair strategy, introduced by Todoroki and Haftka (1998), is applied with modifications to handle the given constraints which are requirements of balanced laminate construction (balance constraint) and a limit of four contiguous plies with the same fiber orientation (four-contiguity constraint). In the current study, the repair strategy is modified to satisfy the given constraints in all three regions shown in Fig. 3. The continuous sublaminate satisfies the balance constraint, thus the dropped plies also must be balanced. Moreover, four-contiguity constraint must be satisfied before and after tapering.

For the problem with multiple global optima, the optimization process that finds as many optima as possible is required. To accomplish this requirement, multiple elitism, which copy the best designs in current generation into the next generation are adopted. The works of Cho and Rhee (2003, 2004) showed that a

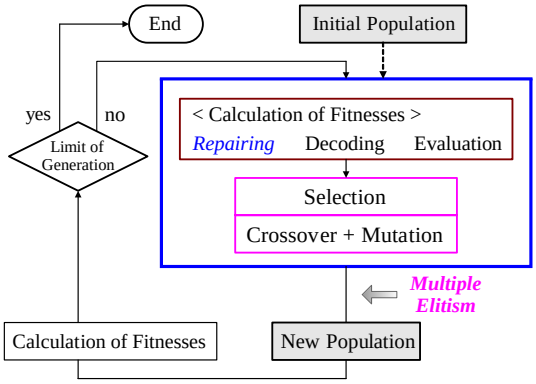

Fig. 6. Flowchart of genetic algorithm with a repair strategy and multiple elitism.

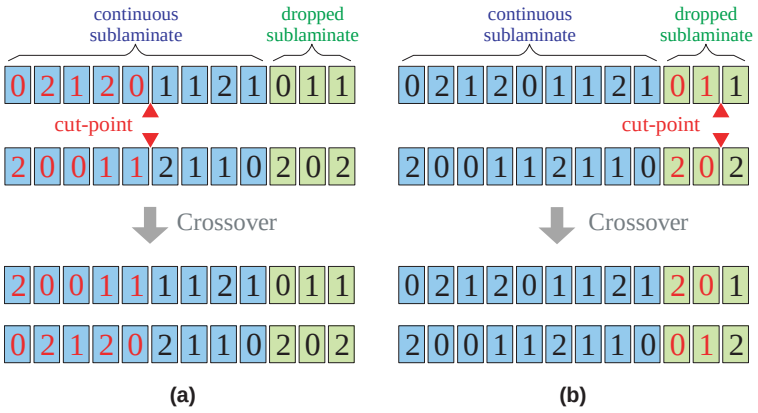

Fig. 7. Crossover scheme using one cut-point: (a) cut-point on the continuous sublaminate, (b) cut-point on the dropped sublaminate.

GA module with a repair strategy and multiple elitism is efficient for the layup optimization considering free-edge strength.

3.2. Multiple elitism

The schematic of multiple elitism is shown in Fig. 8. The top designs (elites) from the parent population are selected and placed into the new population. The child designs required to fill the remainder of the new population are created from the remaining parents that have not been selected as multiple elites, and then placed into the new population. This selection scheme is computationally less intensive because fewer child designs require fitness computation. The number of elites to be copied into the next generation (N_e) is determined by the following equation, in which the more elites are selected as the population size increases:

$$N_e = \left\lfloor \frac{\text{PopSize} + 10}{7} \right\rfloor \tag{25}$$

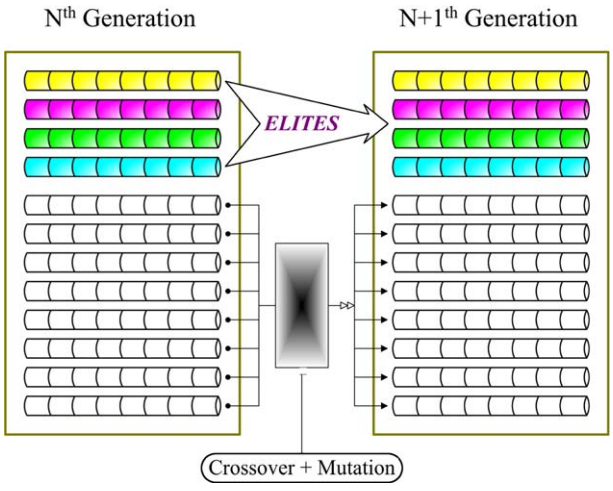

Fig. 8. Schematic of multiple elitism.

where PopSize is the population size and the symbol "$\lfloor\ \rfloor$" (floor) indicates the largest integer smaller than or same as the number in the symbol. For example, when population size is 25, five elites are selected and copied into the next generation.

3.3. Criteria to evaluate the performance of GA with multiple elitism

If the optimized results have been obtained, the performance of GA can be estimated for various population sizes. In the following study, four different criteria, which were previously proposed by Soremekun et al. (2001), are applied to assess the performance of the present GA. The first criterion is the normalized cost per genetic search, C_n, determined by

$$C_n = \frac{N_g N_c}{R}\left(R = \frac{N_{op}}{N_r}\right) \tag{26}$$

where N_g is the number of generations per run, N_c is the number of child designs created in each generation, and R is reliability. If GA is run N_r times and succeeds in finding at least one of the several global optima N_{op} times of these runs, then the reliability R is calculated as the equation in the parenthesis of Eq. (26).

The second criterion is the average number of optima found per genetic search

$$A_{N_0} = \frac{\sum_{i=1}^{N_r} N_o^i}{N_r} \tag{27}$$

where N_o^i is the number of optima found in the ith optimization run.

The third criterion is defined as the cost per optimum found:

$$C_o = \frac{N_g N_c}{A_{N_0}} \tag{28}$$

Table 1
Various parameters used in the application of GA

Parameters	Values
Chromosome length	12
Upper limit of generation	250
Number of runs (N_r)	20
Population size	10–120
Probability of mutation	0.1
Probability of crossover	0.95

Table 2
Optimum layups and their fitness values (without eccentricity)

Loading	Optimum layups		Fitnesses (N/m)
	Continuous sublaminate	Dropped sublaminate	
Shearing (N_{xy})	$[0/45/0/90/-45/\pm45_2]$	$[90_2/0]_s$	9.7633×10^5
	$[90/45/0/90/-45/\pm45_2]$	$[90_2/0]_s$	9.7616×10^5
	$[0/45/90/0/-45/\pm45_2]$	$[90_2/0]_s$	9.7489×10^5
Compression (N_{yy})	$[0/90_2/45/0/90_3/-45]$	$[0/\pm45]_s$	1.2067×10^6
	$[0/90_2/45/0/90_3/-45]$	$[45/0/-45]_s$	1.2062×10^6
	$[0/90/45/0_2/-45/90_2/0]$	$[45/0/-45]_s$	1.1955×10^6

The final criterion is the final population richness, which helps to monitor how the GA exploits global optimum regions of the design space. Final population richness p_r is defined as

$$p_r = \frac{N_{\Delta f}}{\text{PopSize} \cdot N_r} \tag{29}$$

Table 3
Optimum layups and their fitness values (with eccentricity)

Loading	Optimum layups		Fitnesses (N/m)
	Continuous sublaminate	Dropped sublaminate	
Shearing (N_{xy})	$[\pm 45_3/45/90/-45]$	$[90_2/0]_s$	1.2026×10^6
	$[\pm 45_3/45/90/-45]$	$[90_2/0/90]_s$	1.1905×10^6
	$[\pm 45_3/45/90/-45]$	$[0/90/0]_s$	1.1717×10^6
Compression (N_{yy})	$[45/90_3/-45/90_2/0/90]$	$[\pm 45/0]_s$	1.9749×10^6
	$[90/45/90_3/-45/90/0/90]$	$[\pm 45/0]_s$	1.9747×10^6
	$[45/90_3/-45/90_2/0/90]$	$[45/0/-45]_s$	1.9745×10^6

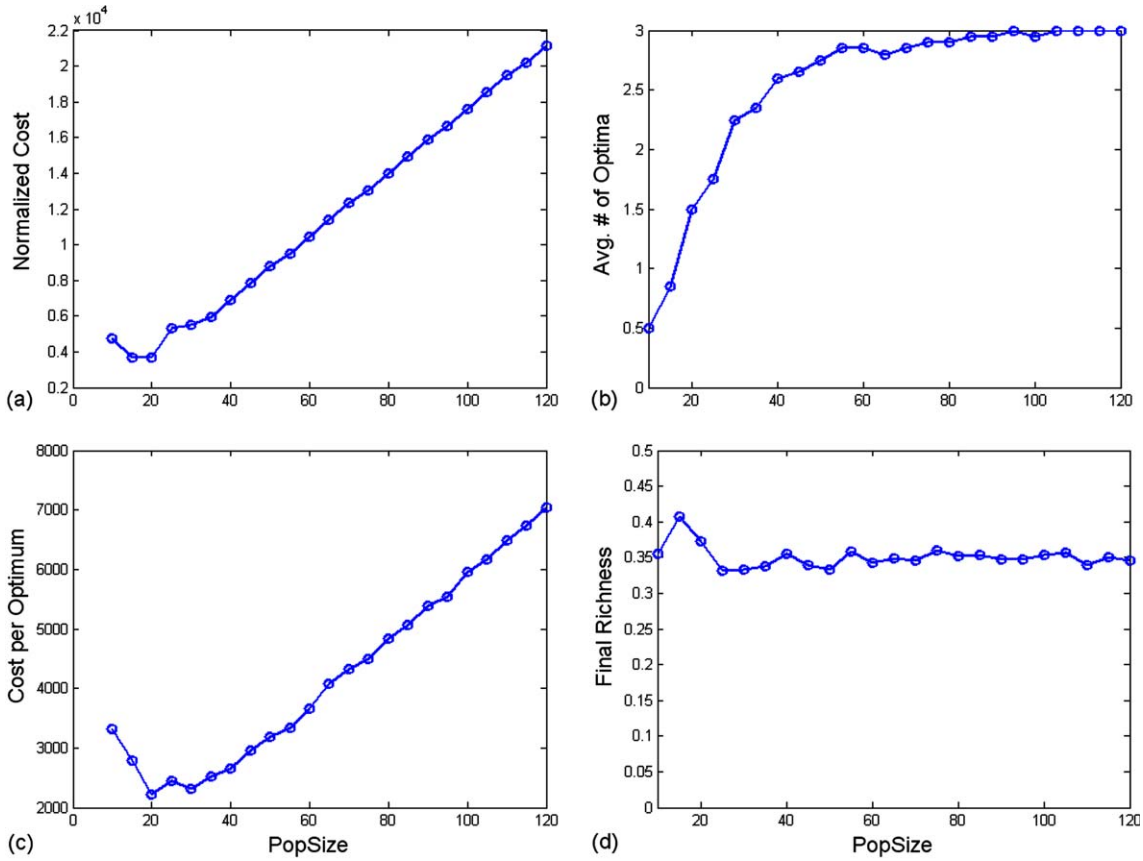

Fig. 9. Performance of GA for various population sizes under the shear loading (without eccentricity).

where $N_{\Delta f}$ is the number of members in the final population of each run with fitness values within a certain small amount (Δf) of the optimum.

4. Results of optimization

The layup optimization for the maximum strength of the laminate without or with eccentricity was executed for the cases of shear loading and compression. In the calculation of the interlaminar stresses, two-term expansion ($n = 2$) in Eq. (5), is used. These selections are sufficient to obtain accurate stresses. The layup of dropped plies as well as that of continuous sublaminate is coded into a chromosome, i.e., a chromosome represents the continuous nine-ply sublaminate and half of the dropped six-ply sublaminate. Thus the length of chromosome is twelve. The present analysis module can calculate the interlaminar stress distributions for one layup within 0.7 s by using the computer with 3.4GHz Pentium IV CPU and 1GB RAM.

Material properties and allowable stresses are adopted from the Eqs. (23) and (24). Various parameters—population size, probability of mutation, and probability of crossover, and so on—are given in Table 1. From authors' experience, the cases with lower probability of mutation are better than those with higher probability and the reliable range of the probability is from 0.05 to 0.25. In the present work, the probability of mutation is chosen as 0.1. The three optimum layups, which we wish to find, and their fitness values

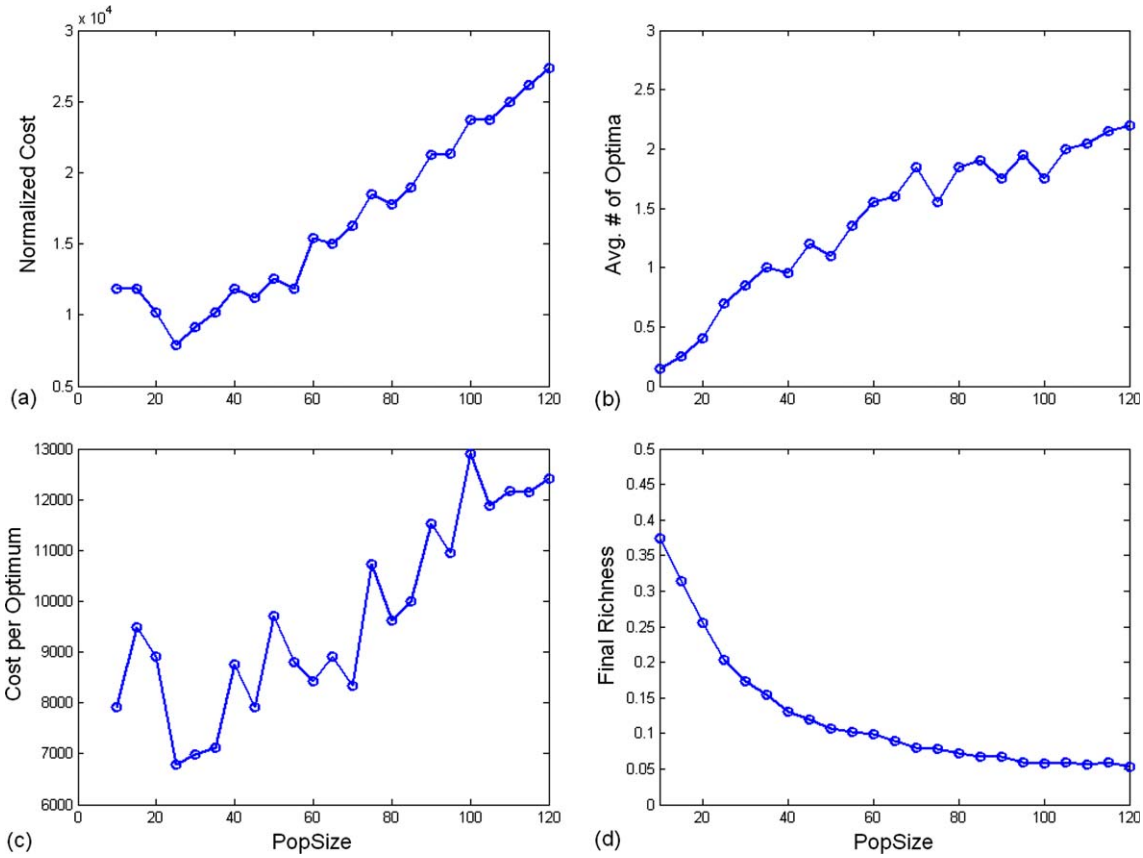

Fig. 10. Performance of GA for various population sizes under the compressive loading (without eccentricity).

are summarized in Tables 2 and 3. To evaluate $N_{\Delta f}$ in Eq. (29), we consider the designs whose fitnesses are within the deviation of about 8% from the optimal one. The numerical performances of GA for the cases of the geometry without eccentricity are plotted for the various population sizes in Fig. 9 under the shear loading and in Fig. 10 under the compressive loading. Those for the cases of the geometry with eccentricity are plotted in Fig. 11 under the shear loading and in Fig. 12 under the compressive loading. Each left two figures are related with the cost of GA, and the right upper figure shows the average number of optima found per genetic search, and the right lower one is for the final population richness. As the population size gets larger, the GA requires more cost but finds more optima. By the implementation of the multiple elitism, the average number of optima could be converged to the maximum value 3 for the cases of shear loading. However, for the compression loading cases, contrary to expectation, the GA could not find all three multiple optima but found only two, because the third optimum layup has somewhat peculiar pattern of continuous sublaminate compared with other optima for the case of "without eccentricity". Similarly, for the case of "with eccentricity", the second optimum has somewhat different pattern of continuous sublaminate from other optima. Thus the last population has more chance to contain two optima, one of which is from two similar layup optima and the other of which is the optimum with different pattern layup.

Figs. 13 and 14 show the number of iterations in which each global optimum could be found. The best, the second and the third optimum layups are represented by asterisk, circle and square, respectively. As the population size becomes larger, all three multiple optima could be found in almost every run for the shear

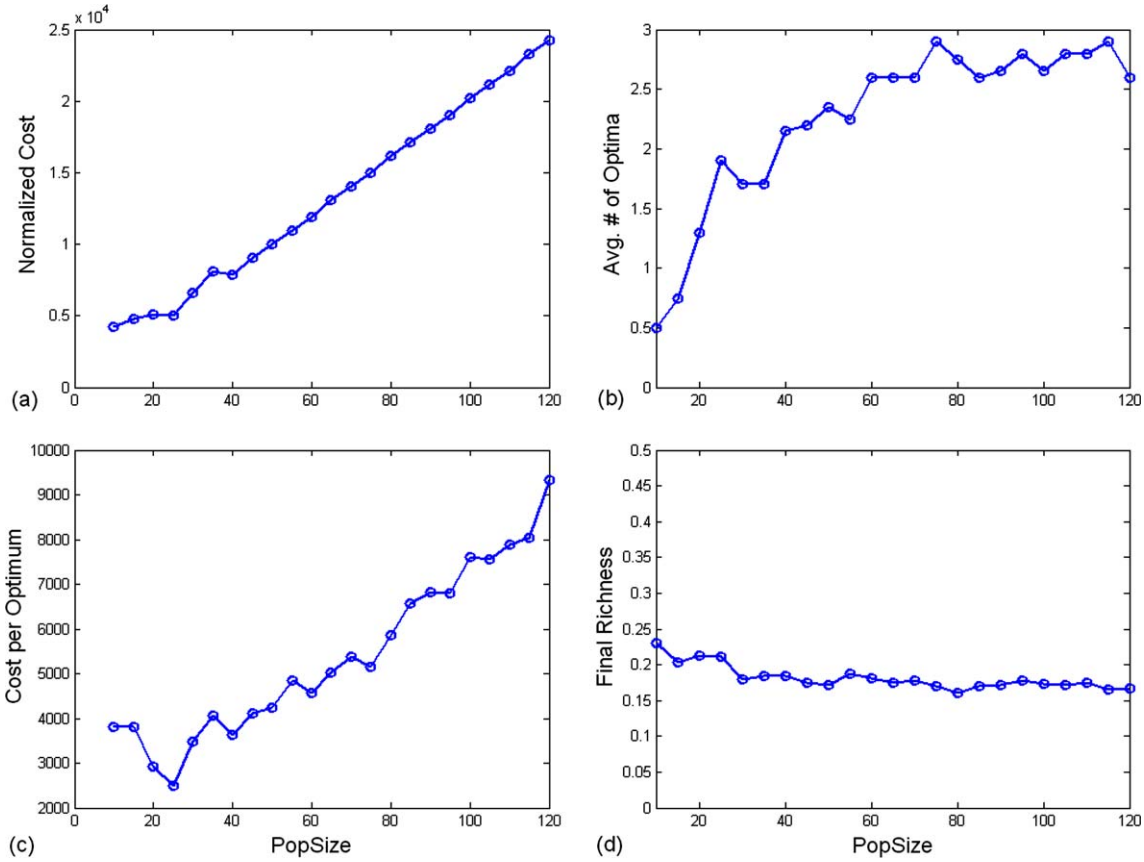

Fig. 11. Performance of GA for various population sizes under the shear loading (with eccentricity).

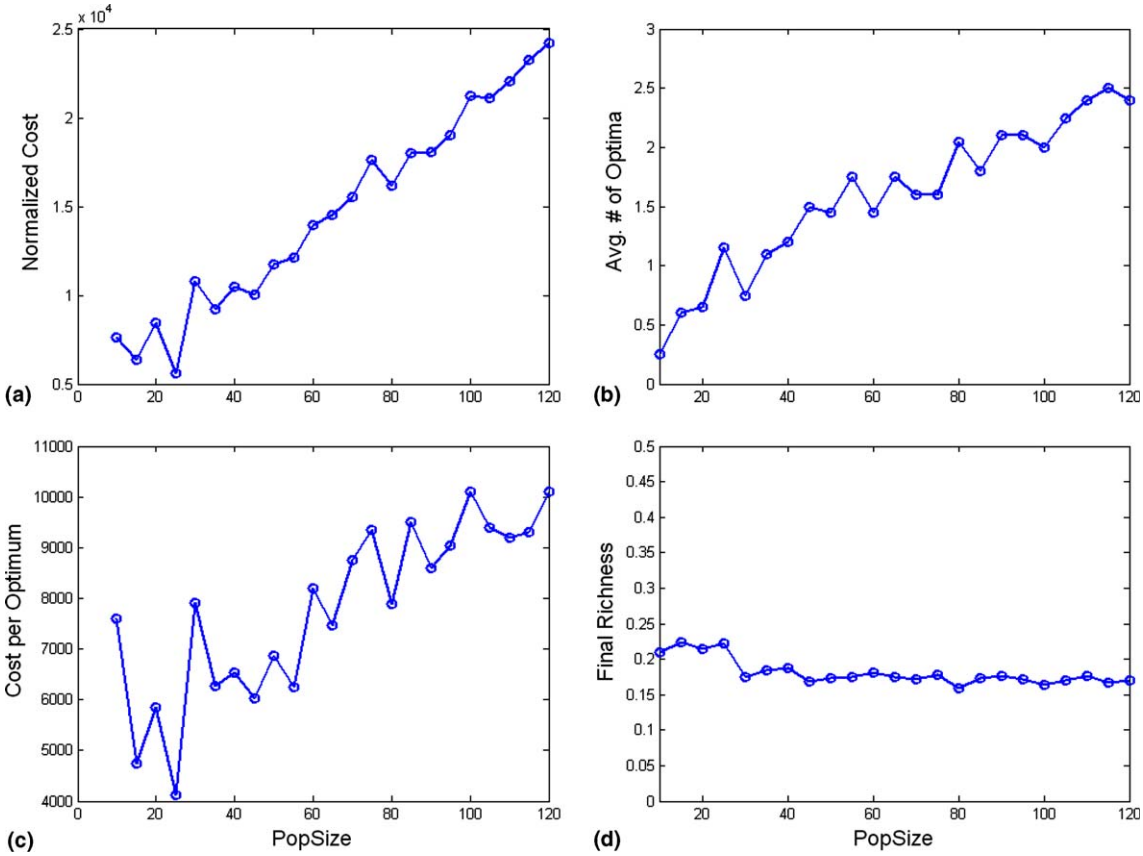

Fig. 12. Performance of GA for various population sizes under the compressive loading (with eccentricity).

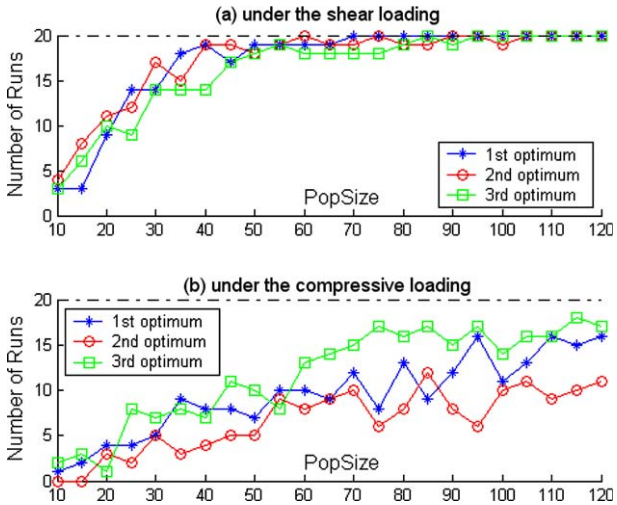

Fig. 13. Number of iterations in which each global optimum could be found (without eccentricity).

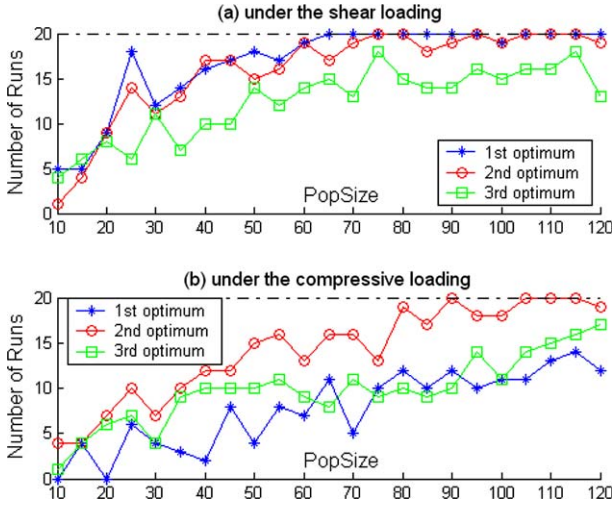

Fig. 14. Number of iterations in which each global optimum could be found (with eccentricity).

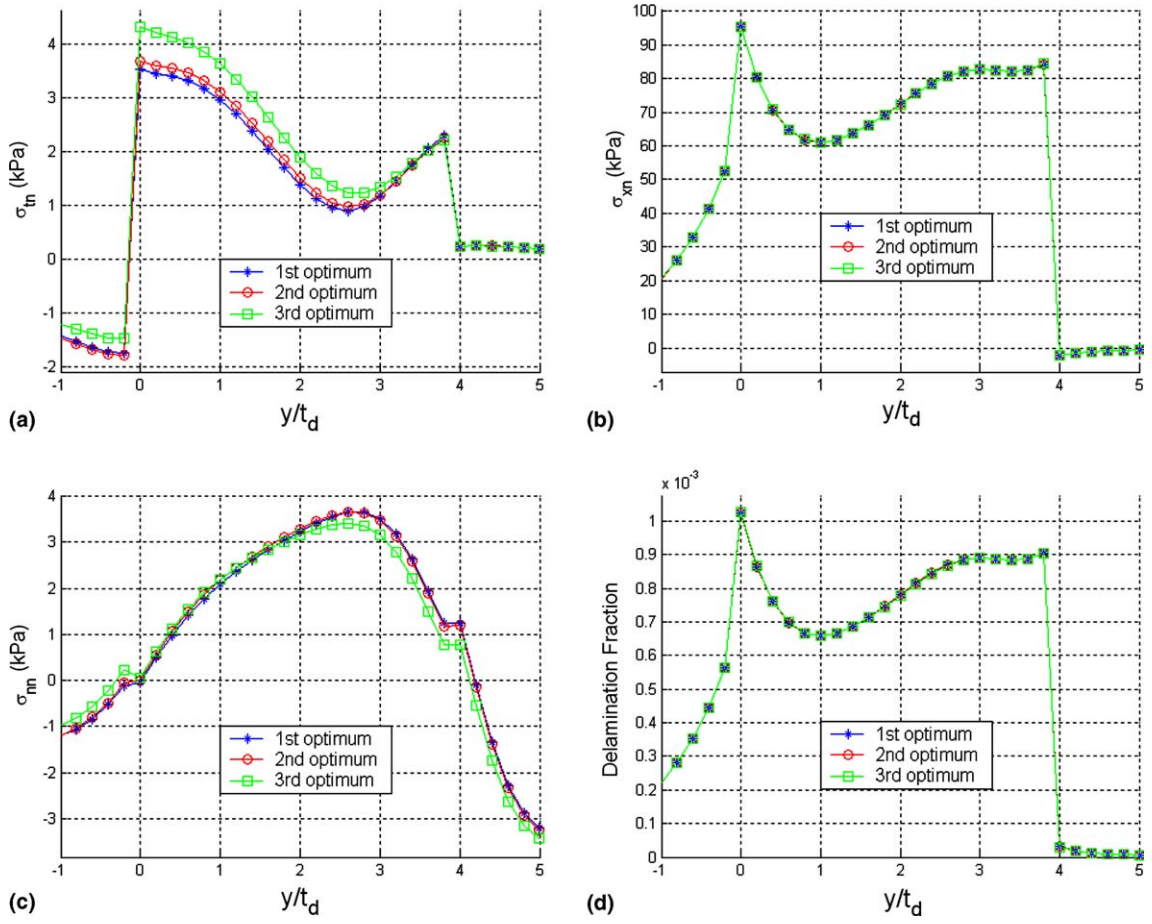

Fig. 15. Interlaminar normal/shear stresses and delamination fraction in the optimum layups under the shear loading (without eccentricity).

loading case. For the compressive loading case, all three multiple optima could not be found by a single run, but could be obtained in a number of iterations with a sufficiently large population size. Actually this means a limitation in performance of the present GA optimization module, but in a practical point of view, the probabilistic optimization procedures like GA should be executed in such many times that the reasonability of the results can be assured. Thus, the present GA tool can assure the reasonability of its results.

To promote readers' comprehension, distributions of the interlaminar normal and shear stresses and delamination fraction in the optimum layups are plotted in Figs. 15 and 16 for the case of "without eccentricity", while those for the case of "with eccentricity" are plotted in Figs. 17 and 18. Under the shear loading, delamination fraction is determined mainly due to the interlaminar shear stress σ_{xn} while it is determined by the interlaminar normal stress under the compressive loading. Three optimum layups have similar distribution of delamination fraction under the shear loading, but for the case of compressive loading, one layup has somewhat different delamination fraction distribution from other layups as mentioned before.

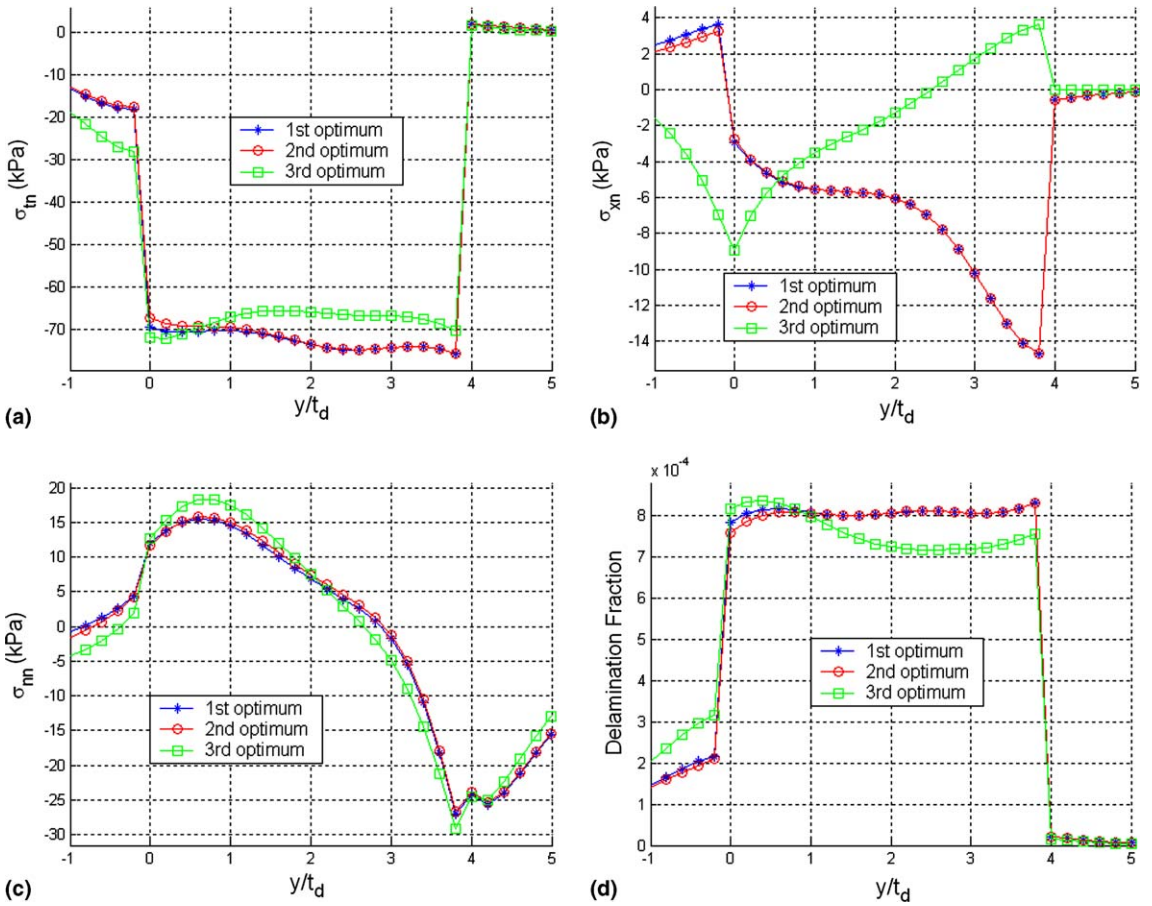

Fig. 16. Interlaminar normal/shear stresses and delamination fraction in the optimum layups under the compressive loading (without eccentricity).

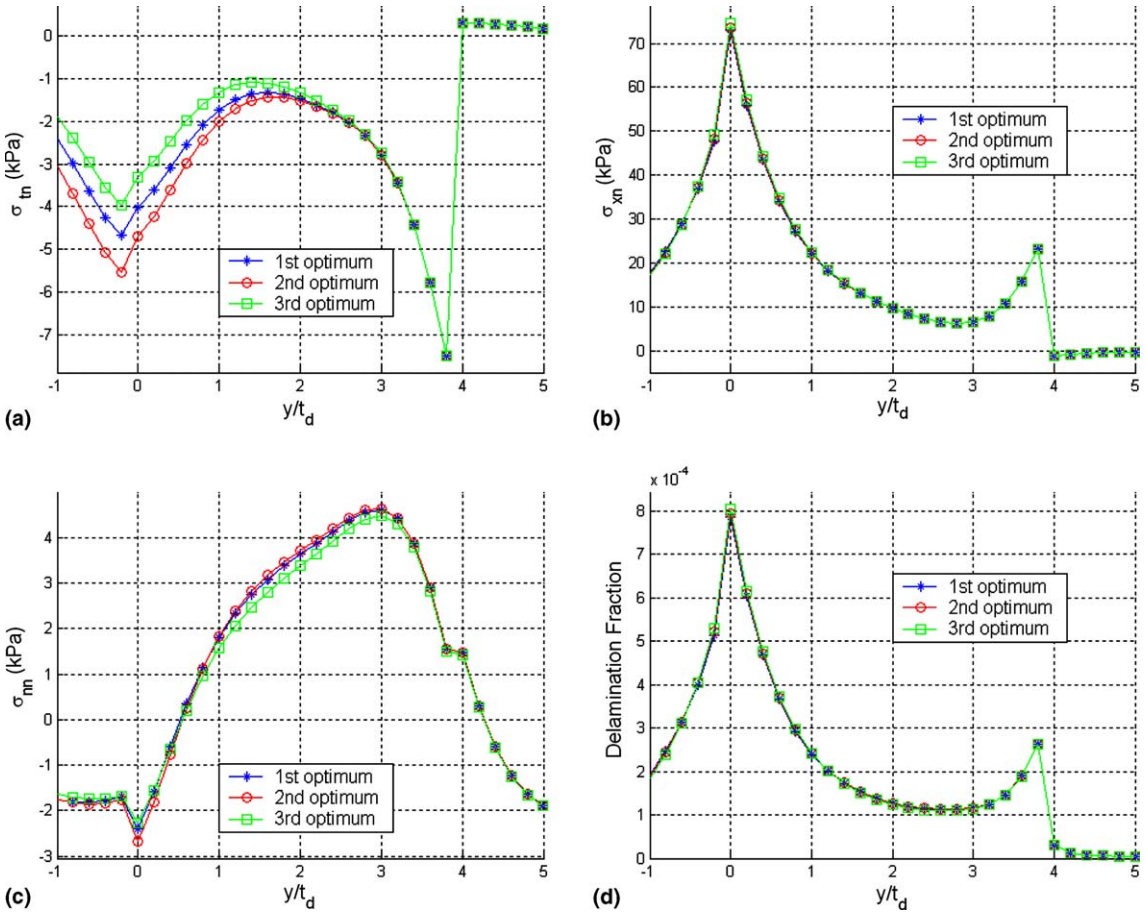

Fig. 17. Interlaminar normal/shear stresses and delamination fraction in the optimum layups under the shear loading (with eccentricity).

5. Conclusion

Layup optimization of the maximum strength of laminated composites with internal ply-drops under longitudinal compression and in-plane shear loading conditions has been performed by genetic algorithm (GA). Interlaminar stresses were obtained by the stress function based complementary virtual work principle. Out-of-plane stress functions were expanded in terms of harmonic series through the thickness direction and initially satisfied the traction free boundary conditions of laminates. The stress function-based complementary virtual work principle was simple and efficient in calculating the interlaminar stresses of the composite laminates with dropped plies. This gave a great potential in the layup optimization for maximum interlaminar strength of the laminates with internal ply-drops. The layup optimization has been conducted by genetic algorithm with repair strategy, which worked well in handling given constraints. The repair strategy was applied in each region before tapering and after tapering. The multiple elitism was able to find more solutions near the global optimum. This is important because the designer could have more flexibility in selecting the layup of composite laminates. However, in compressive loading cases, the present GA cannot find all three optima in a single run but only needs a sufficiently many iterations to find all optima. Thus, the present GA can be applied as an optimization tool in a practical point of view.

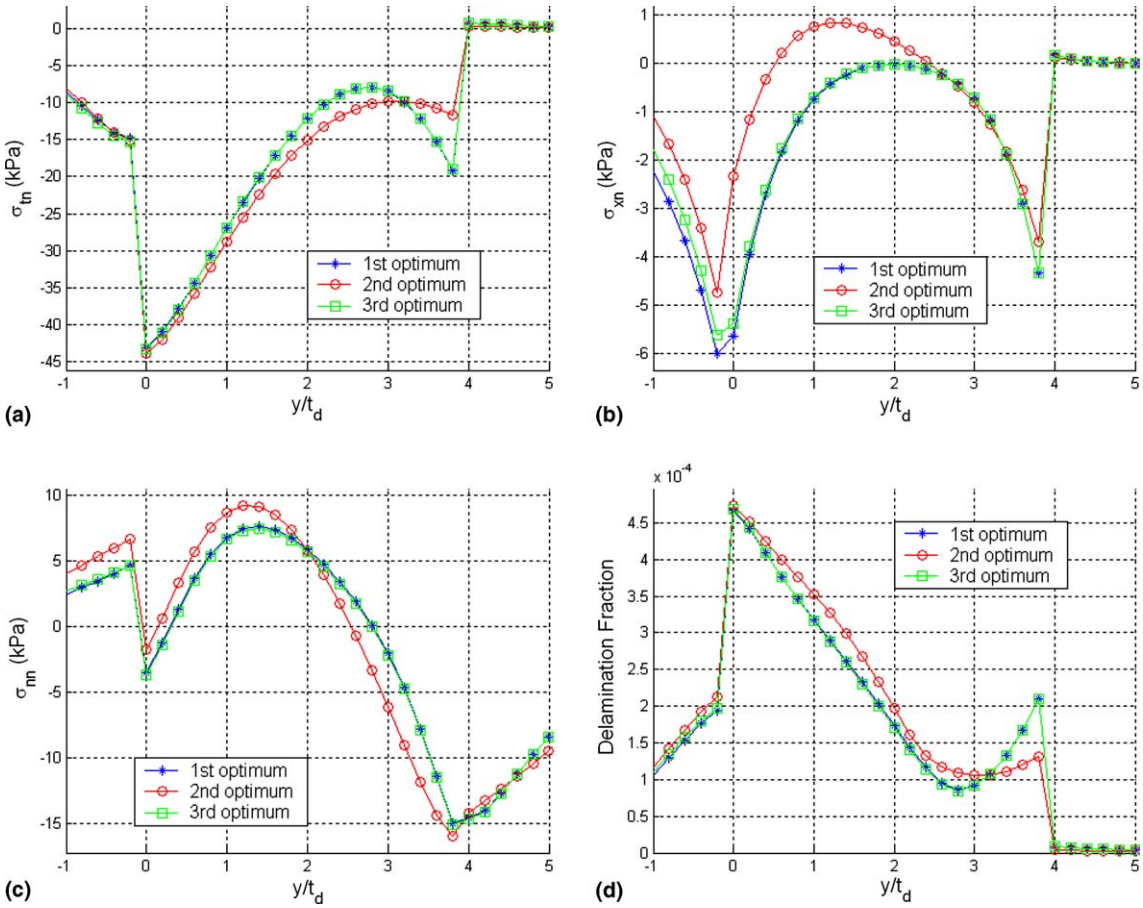

Fig. 18. Interlaminar normal/shear stresses and delamination fraction in the optimum layups under the compressive loading (with eccentricity).

The layup optimization under general loading condition is not performed. Therefore, it is remarked that the layup optimization under general loading conditions such as transverse tensile loading, thermal loading and combined loading will be undertaken as a second phase of this study.

Acknowledgement

This work was supported by the Micro Thermal System Research Center through the Korea Science and Engineering Foundation.

References

Botting, A.D., Vizzini, A.J., Lee, S.W., 1996. Effect of ply-drop configuration on delamination strength of tapered composite structures. AIAA Journal 34 (8), 1650–1656.

Cho, M., Kim, H.S., 2000. Iterative free-edge stress analysis of composite laminates under extension, bending, twisting and thermal loadings. International Journal of Solids and Structures 37 (3), 435–459.

Cho, M., Rhee, S.Y., 2003. Layup optimization considering free-edge strength and bounded uncertainty of material properties. AIAA Journal 41 (11), 2274–2282.

Cho, M., Rhee, S.Y., 2004. Optimization of laminates with free edges under bounded uncertainty subject to extension, bending and twisting. International Journal of Solids and Structures 41 (1), 227–245.

Cho, M., Yoon, J., 1999. Free-edge interlaminar stress analysis in composite laminates by the extended Kantorovich method. AIAA Journal 37 (5), 656–660.

Fish, J.C., Lee, S.W., 1989. Delamination of tapered composite structures. Engineering Fracture Mechanics 34, 43–54.

Harrison, P.N., Johnson, E.R., 1996. A mixed variational formulation for interlaminar stresses in thickness-tapered composite laminates. International Journal of Solids and Structures 33 (16), 2377–2399.

Le Riche, R., Haftka, R.T., 1993. Optimization of laminate stacking sequence for buckling load maximization by genetic algorithm. AIAA Journal 31 (5), 951–956.

Lekhnitskii, S.G., 1963. Theory of Elasticity of an Anisotropic Body. Holden-Day, Inc., San Francisco.

Mukherjee, A., Varughese, B., 1999. Development of a specialized finite element for the analysis of composite structures with ply drop-off. Composite Structures 46, 1–16.

Pipes, R.B., Pagano, N.J., 1970. Interlaminar stresses in composite laminates under uniform axial extension. Journal of Composite Materials 4, 538–548.

Soremekun, G., Gürdal, Z., Haftka, R.T., Watson, L.T., 2001. Composite laminate design optimization by genetic algorithm with generalized elitist selection. Computers and Structures 79, 131–143.

Todoroki, A., Haftka, R.T., 1998. Stacking sequence optimization by a genetic algorithm with a new recessive gene like repair strategy. Composite Part B 29 (3), 277–285.